Blue Intensity based experiments for reconstructing North Pacific temperatures along the Gulf of Alaska

Rob Wilson[1,2]; Rosanne D'Arrigo, [2]; Laia Andreu-Hayles[2]; R. Oelkers,[2]; Greg Wiles[2,3]; Kevin Anchukaitis[4,2] and Nicole Davi[2,5]

1. University of Saint Andrews, Saint Andrews, UK; **2.** Tree-Ring Laboratory, Lamont-Doherty Earth Observatory, Palisades, NY, USA; **3**. The College of Wooster, Wooster, Ohio; **4.** School of Geography and Development & Laboratory of Tree Ring Research, University of Arizona, Tucson, AZ USA **5.** William Paterson University, New Jersey, USA.

To be Submitted to Climate of the Past

Abstract: Ring-width (RW) records from the GOA have yielded a valuable long-term perspective for North Pacific changes on decadal to longer time scales in prior studies, but contain a broad winter to late summer seasonal climate response. Similar to the highly climate-sensitive maximum latewood density (MXD) proxy, the Blue Intensity (BI) parameter has recently been shown to correlate well with year-to-year warm-season temperatures for a number of sites at northern latitudes. Since BI records are much less labor intensive and expensive to generate than MXD, such data hold great potential value for future tree-ring studies in the GOA and other regions in mid-to-high latitudes. Here we explore the potential for improving tree-ring based reconstructions using combinations of RW and BI-related parameters (latewood BI and delta BI) from an experimental sub-set of samples at eight mountain hemlock (*Tsuga mertensiana*) sites along the GOA. This is the first study for the hemlock genus using BI data. We find that using either inverted latewood BI (LWB_{inv}) or delta BI (DB) can improve the amount of explained temperature variance by > 10% compared to RW alone, although the optimal target season shrinks to June-September, which may have implications for studying ocean-atmosphere variability in the region. One challenge in building these BI records is that resin extraction did not remove colour differences between the heartwood and sapwood, so long term trend biases, expressed as relatively warm temperatures in the 18th century, were noted when using the LWB_{inv} data. Using DB appeared to overcome these trend biases resulting in a reconstruction expressing 18th-19th century temperatures ca. 0.5^{o}C cooler than the 20th/21st centuries. This cool period agrees well with previous dendroclimatic studies and the glacial advance record in the region. Continuing BI measurement in the GOA region must focus on sampling and measuring more trees per site (> 20) and compiling more sites to overcome site-specific factors affecting climate response and using sub-fossil material to extend the record. Although LWB_{inv} captures the inter-annual climate signal more strongly than DB, DB appears to better capture long term secular trends that agree with other proxy archives in the region. Great care is needed, however, when implementing different detrending options and more experimentation is necessary to assess the utility of DB for different conifer species around the Northern Hemisphere.

Keywords: Blue Intensity, Gulf of Alaska, Tree Rings, Reconstruction, North Pacific**; Short Title**: Gulf of Alaska Blue Intensity Tree-Ring Temperature Reconstruction

1. Introduction

The climate of the Gulf of Alaska (GOA) is strongly influenced by the atmosphere-ocean variability of the North Pacific sector (e.g. the Pacific Decadal Oscillation, Mantua et al. 1997), with profound socioeconomic implications for the region (Ebbesmeyer et al. 1991). The variability of such synoptic climate phenomena is more strongly expressed in winter. Ring-width (RW) data measured from montane treeline conifer trees in the GOA region often express a broad seasonal response window (e.g. January-September, Wilson et al. 2007; February-August, Wiles et al. 2014), which has allowed such data to provide information on cold season synoptic dynamics covering almost two thousand years (Barclay et al. 1999, D'Arrigo et al. 2001, Wiles et al. 2004 and 2014, Wilson et al. 2007).

Maximum-latewood density (MXD) measurements have yielded long records of past summer temperatures for many regions in the northern mid-to-high latitudes (e.g. Schweingruber 1988, Briffa et al. 2002, Anchukaitis et al. 2013, Schneider et al. 2015), but such records do not yet exist for the GOA. MXD series are particularly desirable as such records often have stronger correlations with temperatures than RW and result in climate reconstructions with better skill and spectral fidelity (Anchukaitis et al. 2013, Esper et al. 2015, Wilson et al. 2016, Anchukaitis et al. 2017). This is partly because RW chronologies typically exhibit higher autocorrelation and lagged memory effects than MXD (Briffa et al. 2002; Anchukaitis et al. 2012), but also because RW may potentially integrate other ecological signals (e.g. disturbance and stand dynamics) which can

62 obscure the climate signal (Rydval et al. 2015). Yet, only two millennial-length MXD records are
63 currently published for all of north-western North America (Icefields, British Columbia (BC),
64 Canada - Luckman and Wilson 2005; Firth River, Alaska - Andreu-Hayles et al. 2011, Anchukaitis
65 et al. 2013) and no MXD data have been generated to date for the entire GOA. This situation
66 partly relates to the expensive and labor intensive nature of MXD measurement, but also because
67 the wood of mountain hemlock (*Tsuga mertensiana*), a dominant conifer species in the GOA, is
68 rather brittle and does not lend itself well to standard sample preparation for MXD measurement.
69
70 To help meet the need for additional climatically-sensitive density records from north-western
71 North America, we present herein an exploration of novel Blue Intensity (BI) parameters measured
72 from scanned images of tree core samples from the GOA. Minimum latewood blue intensity
73 (LWB) has recently been shown to have strong similarities to MXD, and is much cheaper and
74 simpler to generate (McCarroll et al. 2002; Björklund et al. 2014, 2015; Rydval et al, 2014; Wilson
75 et al. 2014, 2017). LWB is closely related to MXD as they both measure similar wood properties
76 (combined hemicellulose, cellulose and lignin content related to cell wall thickness), and both are
77 well correlated with warm-season temperatures (Campbell et al. 2007; Björklund et al. 2014,
78 Rydval et al. 2014, Wilson et al. 2014). This correspondence between BI and temperature has
79 recently been shown to hold true for several locations and tree species, including Scots pine (*Pinus*
80 *sylvestris*) in Scotland, UK (Rydval et al. 2014) and Sweden (Björklund et al. 2014, 2015),
81 Caucasian fir (*Abies nordmanniana*) in the Northern Caucasus' (Dolgova 2016), Stone pine (*Pinus*
82 *cembra*) in Austria (Wilson et al. 2017), Engelmann spruce (*Picea engelmannii*) from the Canadian
83 Rockies, British Columbia, Canada (Wilson et al. 2014) and our own analyses of white spruce
84 (*Picea glauca*) in north-western North America (Andreu-Hayles et al., ms. in prep.). Although BI

85 often requires larger sample sizes than MXD to improve signal strength (Wilson et al. 2014), this
86 is not a concern due to the low cost of the method.
87
88 The greatest limitation of LWB, however, is that any colour variation that does not represent year-
89 to-year climate-driven cell wall thickness changes will bias the resultant raw reflectance
90 measurements. For example, some conifer species (including Scots pine and mountain hemlock)
91 show a clear sharp or transitional colour change from the heartwood to sapwood, which, even after
92 resin extraction using ethanol or acetone, can still impose a systematic change in reflectance
93 around the heartwood/sapwood transition (Rydval et al. 2014; Björklund et al. 2014, 2015). Further
94 colour variations, often seen in dead but preserved snag or sub-fossil wood, can also result in
95 systematic biases when combined with data measured from living samples (Björklund et al. 2014,
96 2015; Rydval et al. 2014). Björklund et al. (2014) proposed a potential solution to the
97 heartwood/sapwood colour bias issue by effectively detrending the LWB measurements by
98 removing the inherent common colour changes of the earlywood and latewood (i.e. those related
99 to heartwood/sapwood colour change). This is accomplished by subtracting the raw LWB value
100 from the maximum blue reflectance value of the earlywood (EWB) for each year. The resulting
101 new parameter, delta blue intensity (hereafter referred to as DB), should theoretically be less biased
102 by such non-climatic related colour changes. Although Björklund et al. (2014, 2015) presented
103 compelling results using Scots pine in Sweden, DB has not yet been tested elsewhere or on any
104 other species.
105
106 Finally, although BI based variables hold great promise as an alternative proxy to MXD, another
107 potential concern is the possibility that reflectance based measurements may not capture low

frequency information related to long term-climate changes. Wilson et al. (2014), working with Engelmann spruce from British Columbia, which does not have a visual colour difference between the heartwood and sapwood, urged caution as both the MXD and LWB parameters were sensitive to different detrending options and there was some indication that LWB could not capture as much low frequency information as MXD. However, this observation could not be fully addressed due to the relatively short instrumental record in British Columbia.

In this paper, building upon previous RW based research (Wilson et al. 2007, Wiles et al. 2014), we measure BI variables (EWB, LWB and DB) from multiple sites in the GOA to evaluate: (a) whether BI can improve on previous RW-only based reconstructions, and (b) whether meaningful low frequency information can be gleaned from these data by exploiting the long monthly instrumental record from Sitka, Alaska back into the mid-19th century to validate secular trends in the TR data.

2. Methods and Analysis

For this exploratory study, BI measurements were made on a subset (ca. 15 single tree cores per site) of crossdated core samples collected over the past few decades from living mountain hemlock (*Tsuga mertensiana* Bong. Carrière) trees located at eight sites near altitudinal treeline (approximately ~300-400 meters above sea level) along the GOA (Table 1, Figure 1). Data from these and additional sites were used previously to create coastal GOA RW based temperature-related reconstructions (D'Arrigo et al. 2001, Wilson et al. 2007, Wiles et al. 2014).

The tree core samples were immersed in acetone for 72 hours to remove excess resins in the wood (Rydval et al. 2014) and then finely sanded to 1200 grit to remove marks and abrasions prior to scanning. An Epson V850 pro scanner, using an IT8.7/2 calibration card in conjunction with Silverfast scanning software, was used to scan the samples at 2400 dpi resolution. Raw EWB and LWB variables were measured using CooRecorder 8.1 software (Cybis 2016 - http://www.cybis.se/forfun/dendro/index.htm), which has capabilities to acquire accurate reflectance intensity RGB colour measurements from scanned wood samples (see Rydval et al. 2014). DB values were calculated within CooRecorder by subtracting the raw LWB values from the raw EWB values for each year. Since raw LWB is negatively correlated to MXD (high density 'dark' latewood = low reflectance), values were inverted following the method detailed in Rydval et al. (2014) to allow for LWB (hereafter denoted as LWB_{inv}) to be detrended in a similar way to MXD (see also Wilson et al. 2014). The nature of the DB calculation results in this parameter being positively correlated with LWB_{inv}, so these data could also be theoretically detrended in a similar way. It should be noted that Björklund et al. (2014) proposed that LWB_{inv} should be referred to as maximum latewood blue absorption intensity.

As the mean sample length (Table 1) for all sites was > 200 years, for initial experiments comparing the different tree-ring (TR) variables, the RW, LWB_{inv}, EWB and DB data were detrended using fixed 200-year cubic smoothing splines (Cook and Peter 1981) to retain the interannual to multi-decadal signal and minimize any potential lower frequency biases due to heartwood/sapwood colour changes. The variance of the site and regional composite chronologies were temporally stabilized using techniques detailed in Frank et al. (2007a). These chronology versions were assessed by (1) signal strength statistics: both common signal (via mean inter-series

155 correlation – RBAR) and expressed population signal (EPS - Wigley et al. 1984) statistics, (2)
156 between variable correlation, (3) between site coherence using a rotated principal component
157 analysis (PCA, varimax rotation using correlation matrices with eigenvectors retained with an
158 eigenvalue > 1.0) and (4) climate response derived by correlations between regional composite TR
159 variable mean series and the dominant PC scores against monthly and season variables of
160 temperature (CRU TS 3.24 (Harris et al. 2012): 57-61°N / 153-134°W).
161
162 The 200-year spline chronology versions were also used to explore calibration (1901-1960) and
163 validation (1961-1989) based principal component regression reconstruction experiments using
164 the CRU TS data. The 1961-1989 period was specifically used for validation as many tree-ring
165 width based temperature sensitive chronologies in Alaska do not track recent temperature trends
166 well – a phenomenon often referred to as the "Divergence Problem" (D'Arrigo et al. 2008). For
167 the PCA, a reasonably replicated common period (1792-1989) was used where tree series
168 replication was > 5 trees. All site chronologies are replicated with > 10 trees from 1792 except for
169 JM and SR (see Table 1) where replication is 6 and 5, respectively. Reconstruction validation was
170 performed using the Pearson's correlation coefficient (r), the Reduction of Error (RE) and the
171 Coefficient of Efficiency (CE - Cook et al., 1994). Further validation was performed over the 1850-
172 1900 period using the gridded BEST instrumental data (Rohde et al., 2012), extracted for the same
173 region as the CRU TS (57-61°N / 153-134°W), after these data were scaled to the CRU TS data
174 over the 1901-2015 period. CRU TS and BEST are compared (Supplementary Figure S1) to the
175 original GOA 5-station mean records used in Wilson et al. (2007) to confirm that the gridded
176 products are good representations of the regional temperature signal. The higher variance of the
177 pre-1950 period in the 5-station mean is related to the fact that variance stabilization (Frank et al.

178 2007a) was not performed when this mean series was originally developed (Wilson et al. 2007)
179 and is therefore likely a less robust measure of GOA temperatures than the gridded products.
180
181 Finally, to improve overall expressed signal strength and explore the potential of reconstructing
182 robust low frequency temperature changes in the region, the data from each of the eight sites were
183 pooled to derive GOA regional composite records for each of the TR variables. These pooled
184 composite variable datasets, with their greater overall replication, allowed detrending experiments
185 to be performed to ascertain the sensitivity of the final parameter chronologies to different
186 detrending choices. Specifically, RW detrending experiments were performed using (1) STD:
187 negative exponential function or negative or zero slope linear function detrending via division; (2)
188 NEPT: negative exponential function or negative or zero slope linear function detrending via
189 subtraction after power transformation of the raw RW data (Cook and Peters 1997); and (3) RCS:
190 single group regional curve standardization (RCS - Briffa et al., 1996; Esper et al., 2003; Briffa
191 and Melvin 2008) detrending via division. The regional age-aligned curve was smoothed using a
192 cubic smoothing spline (Cook and Peters 1981) of 10% the series length. For each of these three
193 approaches, the 'Signal-Free' (SF - Melvin and Briffa 2008) approach to detrending was also used.
194 Finally, the composite chronologies, also using the SF approach, were also derived using the age
195 dependent spline (ADS) approach introduced by Melvin et al. (2007) to track more complex
196 growth trends that may not be captured well with the STD, NEPT and RCS approaches. These
197 different detrending options resulted in an ensemble of 7 different RW composite chronologies.
198 For LWB_{inv} and DB, as they theoretically should behave more like MXD, which often has a
199 decreasing linear trend, detrending was performed using (1) LINres: negative or zero slope linear
200 function detrending via subtraction - with and without the SF approach; (2) RCSres: single group

RCS detrending via subtraction - with and without the SF approach; and (3) ADSsf: the signal free age dependent spline approach. Overall, for LWB_{inv} and DB, five chronology variants were developed for analysis.

3. Results and Discussion

Common signal within the network

RW has the strongest common signal with a median overall RBAR of 0.44 (8 site range: 0.33 – 0.49 - Table 1), whereas LWB_{inv} and DB both have weaker RBAR values of 0.24. EWB shows the weakest common signal with a median RBAR from the 8 sites of only 0.12. In order of decreasing between-series common signal, the number of trees needed to attain an EPS of 0.85 are 7 (RW), 18 (LWB_{inv} and DB), and 41 (EWB) for each variable respectively. On average, therefore, except for RW, actual replication for the reflectance based parameter chronologies are often lower than would be ideally needed to attain a robust expressed population signal. This is important to keep in mind as it is likely that the experimental calibration results presented herein will improve as replication is increased.

The weak signal strength in EWB compared to RW, LWB_{inv} and DB is also reflected in the PCA. The leading PC for RW, LWB_{inv} and DB explains 59%, 53% and 57% of the overall variance, respectively, while just 39% is explained by the EWB PC1. In general, the loadings (based on a varimax rotation) of the chronologies on each PC for each variable are related to the geographical locations across the GOA with PC1 representing the eastern sites and PC2 the western ones (Figures 1 and 2). A similar spatial distribution of loadings was noted in Wilson et al. (2007) using RW data from 31 living sites across the GOA.

224

225 **Seasonal temperature sensitivity**

226 EWB contains a weak response to summer temperature variability with almost no late summer
227 temperature signal (Figure 2) although some significant correlations (r = ~0.3 - 0.4) are found with
228 May and previous October/November temperatures (supplementary Figure S2). Correlations with
229 seasonal temperatures, after 1st differencing, identifies no significant response (supplementary
230 Figure S3). In agreement with previous work (Wilson et al. 2007; Wiles et al. 2014), RW correlates
231 well with a broad range of summer seasons (Figure 2), showing positive correlations for nearly all
232 months from January through to September (Supplementary Figure 2) with June returning the
233 strongest correlation. Correlations do weaken when the data are 1st differenced (supplementary
234 Figure S3), but the Wiles et al. (2014) RW composite still retains a strong response with February-
235 August temperatures although for the other RW based time-series, the summer season shows the
236 strongest coherence. LWB_{inv} and DB, show a weaker response with the late winter/spring months
237 compared to RW and strongest correlations with June, July and August (Figure 2). These
238 observations were expected as LWB_{inv} and DB should express similar growth/climate response
239 properties to MXD.

240

241 For the RW, LWB_{inv} and DB data, there appears to be a geographical difference in response with
242 PC1 (eastern sites) showing stronger seasonal (Figure 2) and monthly (supplementary Figure S2)
243 correlations with temperature than PC2 (western sites). However, correlations of the individual
244 site chronologies for each TR variable (Table 2) against June-September temperatures (optimal
245 season for reconstruction – see later) suggest that there is a degree of variability of the individual
246 sites' response to summer temperatures across the GOA. As PC2 is weighted more towards the

247 TBB site (see PCA loadings in Figure 2 for RW, LWB_{inv} and DB) which correlates weakly with
248 JJAS, it is therefore not surprising that this PC correlates weakly with summer temperatures. After
249 1st differencing, however, these regional differences disappear (supplementary Figure S3)
250 suggesting there are potential post-detrending trend biases in the chronologies weighted on PC2.
251
252 It is important to note that the correlation of the mean composite chronologies with summer
253 temperatures (Figure 2 and especially supplementary Figure S3 after a 1st differenced
254 transformation) are stronger than the PC1 results. This suggests that a regional mean composite
255 approach is potentially optimal in the context of deriving a GOA wide reconstruction which can
256 be extended in the future by data generated from sub-fossil samples.
257
258 The positive correlation of RW, LWB_{inv} and DB to summer temperatures (Figure 2 and Table 2)
259 is also reflected in the inter-correlation between these different variables (Table 3). RW agrees
260 most strongly with DB, followed by LWB_{inv}. EWB, unsurprisingly, has the weakest relationship
261 with the other 3 TR variables. Hereafter, due to the poor signal strength and weak climate signal,
262 the EWB data were not used for further analysis, except in the DB calculations.
263
264 **Calibration/validation experiments**
265 Calibration and validation statistics for various PC regression variable combinations for several
266 summer target seasons are detailed in Table 4 along with results using the GOA RW composite of
267 Wiles et al. (2014). Firstly, calibration of Wiles et al. (2014) to the CRU TS 3.24 data (February –
268 August) over the 1901-1989 period ($r^2 = 0.33$) is stronger than the new RW GOA composite ($r^2 =$
269 0.27) which also shows a significant trend in the model residuals. This residual trend possibly

reflects the fact that there could be a longer term trend missing in the RW data due to the use of 200-year spline detrended chronologies when compared to the RCS processed version of Wiles et al. (2014). Also, the slightly weaker results for the new RW data likely reflect lower replication in the current study compared to Wiles et al. (2014).

The strongest calibration $_{a}r^2$ values for each BI parameter over the 1901-1960 period are 0.49 and 0.47 for LWB_{inv} and DB respectively for the JJA season although DB fails validation with negative RE and CE values over the 1961-1989 period. Minimal model improvement is gained by including RW data. RW+LWB_{inv} calibrates best ($_{a}r^2$ = 0.49) with JJA while RW+DB explains more temperature variance for MJJAS ($_{a}r^2$ = 0.51). However, in both cases, validation RE and CE are negative. Focussing on the full period (1901-1989) calibration, strongest results are found for the JJAS season for all parameter options with $_{a}r^2$ values of 0.27 (RW), 0.43 (LWB_{inv}), 0.38 (DB), 0.38 (RW+LWB_{inv}) and 0.39 (RW+DB) with no 1st order autocorrelation observed for any version. Importantly, only the RW+DB version shows no significant linear trend in the model residuals. The full period (1901-1989) calibrated reconstructions (Table 4) for each of the variable options are presented in Figure 3 along with independent validation (1850-1900) with the BEST gridded data. All parameter iterations fail validation (negative CE values) except for RW+DB which returns positive RE (0.57) and CE (0.19) values. Overall, using this subset of samples from these 8 sites, the calibration results (Table 4 and Figure 3) indicate that BI based parameters explain more temperature variance than using RW alone. However, the fidelity of the resultant reconstructions appears sensitive to the periods of calibration and validation used and it is not clear which of these parameters best represent longer term secular change as the chronologies were limited in the frequency domain by using a fixed 200-year spline detrending option.

293

294 The large-scale climate signal expressed by these data is illustrated by comparing the RW+DB
295 JJAS reconstruction with gridded land/sea HadCRUT4 (Morice et al. 2012; Cowtan and Way 2014
296 – Figure 4a) and land only CRU TS 3.24 (Harris et al. 2012 – Figure 4b) temperatures for the GOA
297 and North Pacific sector. Although the spatial correlations are stronger towards Juneau and Sitka
298 (see Figure 1 for locations) in the east of the region it is clear that these new data represent the
299 temperature variability of the wider GOA region and North Pacific. Continued measurement of BI
300 based parameters from sub-fossil samples taken from across the GOA will allow long term summer
301 temperature variability to be derived for at least the last millennium which will complement the
302 long RW based temperature reconstructions expressing a broader seasonal window (Wilson et al.
303 2007; Wiles et al. 2014).

304

305 **Potential low frequency bias**

306 The main potential limitation to the use of BI based TR variables such as LWB is concerned with
307 low frequency trend biases related to wood colour change. Mountain hemlock, in general, shows
308 darker heartwood and lighter sapwood which resin extraction appears to only minimise but not
309 entirely remove. However, this colour change is not a sharp transition and is expressed in raw
310 EWB and LWB measurements as a steady increase in reflectance intensity. Non-detrended mean
311 composite chronologies of EWB and LWB for the whole GOA region (Figure 5) clearly show the
312 impact of the heartwood/sapwood colour change with increasing intensity values through time (see
313 also Supplementary Figure S4 for a single tree example), especially since the late 18th century. In
314 contrast, MXD generally shows a linear decreasing trend with increasing cambial age (Esper et al.
315 2012). If LWB is indeed a comparable (but inverted) TR variable to MXD as a measure of

316 latewood anatomical density properties, then we would expect, therefore, an increasing trend in
317 raw LWB values. Figure 5 therefore poses a potential "mixed-signal" conundrum as the observed
318 trend in the GOA raw mean LWB composite will incorporate the secular climate signal, the true
319 age-related trend of changing latewood density, and the heartwood/sapwood colour change bias.
320 Although using DB can theoretically overcome the colour bias issue, it has not been explored in
321 any detail beyond the original concept papers (Björklund et al. 2014, 2015). The mean DB non-
322 detrended GOA chronology (Figure 5) has minimal long term trends, which could suggest that the
323 colour change bias has been removed or at least minimised.
324
325 Mean cambial age-aligned curves of the EWB, LWB and DB data show very distinct trends
326 (Supplementary Figure S5). LWB appears to show a general linear increase in values – a trend that
327 would be expected if LWB indeed does reflect similar wood properties (inversely) to MXD. DB,
328 however, has a more complex mean growth curve, essentially reflecting trends in the EWB data,
329 and shows an initial increasing juvenile trend for ~50 years, a period of stabilisation and then a
330 decreasing trend from about ~200 to 300 years. These different age-aligned curves highlight that
331 different detrending options may well be needed for these different TR variables.
332
333 A range of credible options for detrending the RW, LWB_{inv} and DB GOA regional composite data
334 are presented in Figure 6. The outcome for the RW data appears extremely consistent even when
335 using STD vs RCS based methods. However, the LWB_{inv} and DB chronologies are much more
336 sensitive to the detrending method used. Compared to RW and DB, all LWB_{inv} chronology variants
337 show above zero index values in the 18th century, which likely reflects the low reflectance bias of
338 the darker heartwood compared to the sapwood because the LWB_{inv} data have been inverted. The

339 RCS versions appear particularly inflated and as LWB_{inv} is positively correlated with summer
340 temperatures (Figure 2), this would result in markedly warm temperature estimates during the LIA
341 compared to the 20th century which is at odds with previous GOA dendroclimatic analyses (Wiles
342 et al. 2014) and the geomorphological record, which indicate substantial cool conditions and
343 glacial advance from the 17th to 19th centuries (Wiles et al., 2004; Solomina et al. 2016). RCS can
344 impart significant low frequency bias when the assumptions and requirements of the method are
345 not met (Melvin and Briffa 2014; Anchukaitis et al. 2013) and as the GOA composite utilises only
346 living trees, this is a far from optimal sample design for this detrending method. For DB, the LINsf
347 version deviates markedly from LINres, RCSres, RCSsf and ADSsf variants with very low values
348 (< -6 standard deviation from 1901-1989 mean) before 1700 followed by a strong linear increase
349 until present. A similar observation was noted in Wilson et al. (2014) where signal free detrending
350 of LWB_{inv} and MXD resulted in much cooler LIA conditions than other detrending approaches.
351

352 **JJAS GOA summer temperatures back to 1600**

353 The long GOA instrumental record allows for additional assessment of how different reflectance
354 based chronology variants track temperatures back through time. Using the extended BI based
355 regional composite records, further reconstruction experiments against the JJAS season were
356 performed using LWB_{inv} and DB separately (Table 5) by calibrating against JJAS CRU TS3.24
357 (1901-2010) and separately validating using the BEST data (1850-1900). For the LWB_{inv} data, due
358 to their strong post 1970s decreasing trends (Figure 6), RCSres and RCSsf calibrated poorly (Table
359 5: r^2 = 0.07 and 0.05 respectively) and validated with negative CE values over the 1850-1900
360 period. LINres and LINsf explained 41% of the temperature variance while the ADSsf variant
361 explained 47%. All three versions validated reasonably well with positive RE and CE values.

Significant 1st-order autocorrelation (DW range 1.28 to 1.37) and linear trends (LINr range 0.36 to 0.48) were however noted for all model residuals except for ADSsf. For the DB data, calibration was strongest for RCSsf, RCSres and ADSsf with positive RE and CE values for all versions except ADSsf which failed the CE test. The residuals from the RCSsf, RCSres and ADSsf calibrations show no 1st-order autocorrelation although a significant linear trend is observed.

Considering the calibration and validation experiments presented in Tables 4 and 5, our results do not definitively identify whether LWB_{inv} or DB is the optimal BI based parameter for reconstructing past summer temperatures for the GOA region. Part of this ambiguity potentially stems from unknown uncertainties in the 19th century instrumental data, but the sensitivity of the TR parameters to different detrending options (Figure 6) exacerbates the situation. Calibration suggests that the inter-annual based signal of LWB_{inv} is marginally stronger than DB but validation against the 19th century data cannot distinguish between the different parameters. The clear differences between the chronology versions (Figure 6), especially before 1850, have huge implications for understanding past temperatures in the region.

To try and derive a parameter specific view of long term temperature changes for the region, a weighted mean using the five different variants were combined to create a regional average. The r2 values, derived from the 1901-2010 calibration (Table 5), was used as a weighting term to calculate the parameter specific weighted averages which were then calibrated (1901-2010) and validated (1850-1900) in the same way as detailed in Table 5. The resultant weighted LWB_{inv} and DB regional reconstructions report quite different histories of past GOA temperatures (Figure 7). Specifically, the LWB_{inv} reconstruction has temperature estimates from the late 17th to mid-19th

385 century warmer than the 1961-1990 mean, while the DB reconstructions exhibits generally cooler
386 conditions. Both reconstructions explain a similar amount of summer temperature variance
387 (LWB_{inv}: 43% vs. DB: 40%) and validate well with positive RE and CE values. The regression
388 residuals from both versions have a significant linear trend, but only for DB was no significant 1st
389 order autocorrelation identified in the residuals. From comparison to the instrumental data alone,
390 therefore, one cannot objectively identify which of the two parameter versions is most robust.
391 Wilson et al. (2014) highlighted the difficulties of relying solely on the instrumental data to
392 validate the long-term trend in any reconstruction. Moreover, there could be unknown
393 inhomogeneity issues in early instrumental data series which are difficult to identify which would
394 influence calibration and validation (see Frank et al. 2007b). Therefore, alternative sources of
395 relevant information are recommended for further validation. As the geomorphological record in
396 the region suggests a prolonged period of glacial advance occurred in the GOA up to the early 20th
397 century (Wiles et al., 2004; Solomina et al. 2016) when a substantial retreat started, we hypothesize
398 that the pre-1900 period must therefore have been cooler. This would suggest that the DB based
399 reconstruction is likely more representative of past GOA temperatures than the LWB_{inv} driven one.
400
401 Figure 8 presents the RW + DB principal component reconstruction (Figure 3), the weighted
402 LWB_{inv} and DB extended reconstructions (Figure 6), and the Wiles et al. (2014) RW based
403 reconstruction and compares them to the GOA regional glacial advance record (Wiles et al., 2004;
404 Solomina et al. 2016). The LWB_{inv} reconstruction is clearly at odds with the other records with
405 warmer than average temperatures for many periods over the last 400 years and no specific
406 prolonged cooler periods though the LIA. The other TR reconstructions demonstrate centennial
407 and multi-decadal agreement, although the extended DB reconstruction exhibits a smaller

amplitude of temperature change between the LIA period and the 20th century. Overall, temperatures in the GOA region were below the 1961-90 norm throughout most of the LIA with temperatures only rising to substantially higher values in the early 20th century. The coldest decadal periods are centred around the 1700s, 1750s, and 1810s. The glacial advance record shows periods of advance through the LIA, peaking at the end of the 19th century. Despite the use of 200-year spline detrended chronologies, the RW+DB reconstruction has a similar amplitude change to the Wiles et al. (2014) record, which was derived from RCS processed RW data. It should be noted also that this RW based reconstruction was calibrated against Feb-August temperatures which has a greater increasing temperature trend (0.81°C/century vs 0.62°C/century) and higher variance (0.79 vs 0.41) than JJAS (calculated using BEST data from 1850-2015), which will influence the amplitude of the reconstruction (Esper et al. 2005).

4. Conclusions

We have described a set of experimental temperature reconstructions based on RW, LWB_{inv} and DB data measured from eight tree-ring sites along the Gulf of Alaska. Focusing on these data sets, the results demonstrate that inclusion of BI based variables can significantly improve the calibrated variance explained using RW alone by more than 10%.

RW, LWB_{inv} and DB are strongly correlated with each other (Table 3) but the inclusion of LWB_{inv} or DB shifts the calibrated signal from a broad (February-August, Wiles et al. 2014) season using RW alone to a late summer (JJAS) season. The influence of late winter and early spring temperatures on RW suggest that this variable may, in fact, still be the more optimal variable for studying important synoptic phenomena such as north Pacific variability, which dominates in the

winter months (Wilson et al. 2007).

The LWB_{inv} data, for mountain hemlock, despite calibrating and validating in a similar way to DB, are clearly affected by heartwood/sapwood colour differences which impart a trend bias in the resultant chronologies and reconstructions (Figures 6, 7 and 8). However, this bias may not necessarily always occur for other species showing a heartwood/sapwood colour change which could be removed through traditional resin extraction methods. For the first time since the original concept papers by Björklund et al. (2014, 2015), we have experimented with the DB variable. The resulting reconstruction agrees well with a previous RW based reconstruction (Wiles et al. 2014) and the glacial advance record (Wiles et al., 2004; Solomina et al. 2016) for the region.

The analyses presented herein must be viewed as a series of experiments to inform dendroclimatologists of possible methodological strategies that need to be considered for improving TR based reconstructions using BI based variables. Specific to the GOA region, but likely relevant to other regions and species, we therefore detail the following recommendations:

- Although MXD typically has a higher expressed population signal (EPS) strength and climate responses than RW (Wilson and Luckman 2003), signal strength in LWB and DB in GOA hemlock is weaker than RW, so replication needs to be substantially increased (ideally > 20 trees – Table 1) to allow the development of robust chronologies. Rydval et al. (2014) also showed that a substantial improvement in LWB signal strength could be gained by measuring 2 or even 3 radii per tree. Additional assessments of signal strength should be conducted as new species and sites are analysed using BI methods.
- For conifer species with a clear colour difference between the heartwood and sapwood,

454 LWB_{inv} may likely always contain biased long-term trends. The DB variable could
455 potentially minimize this effect as shown here, but more experimentation with this
456 parameter is needed before it can be commonly used as a solution to the LWB_{inv} colour
457 bias problem. Rydval et al. (2017), using Scots pine, overcame the heartwood/sapwood
458 colour bias by utilising a band-pass approach to calibration, where LWB_{inv} drove the
459 decadal and high frequency fraction of the Scottish temperature reconstruction, while RW
460 drove the low frequency variability. This approach however assumes that (1) RW is
461 predominantly controlled by summer temperatures and (2) meaningful long-term
462 information can be gleaned from RW data, which may not always be the case (Esper et al.
463 2012).

464 • There is substantial sensitivity of the final chronologies to varying methodological
465 detrending approaches. Much more exploration of the impact of different detrending
466 choices is needed and it is likely that ensemble based approaches (Wilson et al. 2014) will
467 ultimately be the only way to derive realistic estimates and appropriate detrending based
468 uncertainties bounds. Locations with long instrumental records may help identify more
469 optimal detrending options but care is needed, as it cannot be assumed that the quality of
470 19^{th} century data is comparable to late 20^{th}/early 21^{st} century data. Utilizing other proxy
471 observations of past climate (e.g. in this case the glacial record) may help further constrain
472 TR estimates of past climate especially when different chronology variants (that validate
473 well) portray quite different past temperature histories.

474

475 **Acknowledgments.** This is a contribution to the PAGES 2k Network [through the Arctic/North
476 America-2k working groups]. Past Global Changes (PAGES) is supported by the US and Swiss

National Science Foundations. We also gratefully acknowledge the National Science Foundation's Paleoclimatic Perspectives on Climatic Change (P2C2) Grant Nos. AGS 1159430, AGS 1502186, AGS1502150 and PLR 15-04134. The detailed reviews from Milos Rydval and Jesper Björklund were very much appreciated. Lamont-Doherty Earth Observatory Contribution No. 8121.

5. References

Anchukaitis, K.J., Breitenmoser, P., Briffa, K.R., Buchwal, A., Büntgen, U., Cook, E.R., D'arrigo, R.D., Esper, J., Evans, M.N., Frank, D. and Grudd, H., 2012. Tree rings and volcanic cooling. Nature Geoscience, 5(12), pp.836-837.

Anchukaitis, K.J., D'Arrigo, R.D., Andreu-Hayles, L., Frank, D., Verstege, A., Curtis, A., Buckley, B.M., Jacoby, G.C. and Cook, E.R., 2013. Tree-ring-reconstructed summer temperatures from northwestern North America during the last nine centuries. Journal of Climate, 26(10), pp.3001-3012.

Anchukaitis, K.J., Wilson, R., Briffa, K., Büntgen, U., Cook, E.R., D'Arrigo, R., Davi, N., Esper, J., Frank, D., Gunnarson, B., Hegerl, G., Helama, S., Klesse, S., Krusic, P.J., Linderholm, H., Myglan, V., Osborn, T., Peng, Z., Rydval, M., Schneider, L., Schurer, A., Wiles, G. and Zorita, E. 2017. Last millennium Northern Hemisphere summer temperatures from tree rings: Part II: spatially resolved reconstructions, Quaternary Science Reviews, 163, 1-22, doi: 10.1016/j.quascirev.2017.02.020

Andreu-Hayles, L., D'Arrigo, R., Anchukaitis, K.J., Beck, P.S., Frank, D. and Goetz, S., 2011. Varying boreal forest response to Arctic environmental change at the Firth River, Alaska. Environmental Research Letters, 6(4), p.045503.

Barclay, D.J., Wiles, G.C. and Calkin, P.E., 1999. A 1119-year tree-ring-width chronology from western Prince William Sound, southern Alaska. The Holocene, 9(1), pp.79-84.

506 Björklund, J.A., Gunnarson, B.E., Seftigen, K. and Esper, J., 2014. Blue intensity and density
507 from northern Fennoscandian tree rings, exploring the potential to improve summer temperature
508 reconstructions with earlywood information. Climate of the Past, 10(2), p.877.
509
510 Björklund, J., Gunnarson, B.E., Seftigen, K., Zhang, P. and Linderholm, H.W., 2015. Using
511 adjusted Blue Intensity data to attain high-quality summer temperature information: A case study
512 from Central Scandinavia. The Holocene, 25(3), pp.547-556.
513
514 Briffa, K.R., Jones, P.D., Schweingruber, F.H., Karlén, W. and Shiyatov, S.G., 1996. Tree-ring
515 variables as proxy-climate indicators: problems with low-frequency signals. In Climatic
516 variations and forcing mechanisms of the last 2000 years (pp. 9-41). Springer Berlin Heidelberg.
517
518 Briffa, K.R., Osborn, T.J., Schweingruber, F.H., Jones, P.D., Shiyatov, S.G. and Vaganov, E.A.,
519 2002. Tree-ring width and density data around the Northern Hemisphere: Part 1, local and
520 regional climate signals. The Holocene, 12(6), pp.737-757.
521 Briffa, K.R. and Melvin, T.M., 2011. A closer look at regional curve standardization of tree-ring
522 records: justification of the need, a warning of some pitfalls, and suggested improvements in its
523 application. In Dendroclimatology (pp. 113-145). Springer Netherlands.
524
525 Campbell, R., McCarroll, D., Loader, N.J., Grudd, H., Robertson, I. and Jalkanen, R., 2007. Blue
526 intensity in Pinus sylvestris tree-rings: developing a new palaeoclimate proxy. The Holocene,
527 17(6), p.821.
528
529 Cook ER, Peters K. 1981. The smoothing spline: a new approach to standardising forest interior
530 tree-ring width series for dendroclimatic studies. Tree-Ring Bulletin 41: 45–54.
531
532 Cook, E.R. and Peters, K., 1997. Calculating unbiased tree-ring indices for the study of climatic
533 and environmental change. The Holocene, 7(3), pp.361-370.
534

535 Cowtan, K. and Way, R.G., 2014. Coverage bias in the HadCRUT4 temperature series and its
536 impact on recent temperature trends. Quarterly Journal of the Royal Meteorological Society,
537 140(683), pp.1935-1944.
538
539 D'Arrigo, R., Villalba, R. and Wiles, G., 2001. Tree-ring estimates of Pacific decadal climate
540 variability. Climate Dynamics, 18(3-4), pp.219-224.
541
542 D'Arrigo, R., Wilson, R., Liepert, B. and Cherubini, P., 2008. On the 'divergence problem' in
543 northern forests: a review of the tree-ring evidence and possible causes. Global and Planetary
544 Change, 60(3), pp.289-305.
545
546 Dolgova, E., 2016. June–September temperature reconstruction in the Northern Caucasus based
547 on blue intensity data. Dendrochronologia, 39, pp.17-23.
548
549 Ebbesmeyer, C.C., D.R. Cayan, D.R. McLain, F.H. Nichols, D.H. Peterson and K.T. Redmond,
550 1991:1976 step in the Pacific climate: Forty environmental changes between 1968-75 and 1977-
551 1984. In: Proc. 7th Ann. Pacific Climate Workshop, Calif. Dept. of Water Resources,
552 Interagency Ecol. Stud. Prog. Report 26.
553
554 Esper, J., Cook, E.R., Peters, K. and Schweingruber, F.H., 2003. Detecting low frequency tree-
555 ring trends by the RCS method. Tree-Ring Research, 59(2), pp.81-98.
556
557 Esper, J., Frank, D.C., Wilson, R.J. and Briffa, K.R., 2005. Effect of scaling and regression on
558 reconstructed temperature amplitude for the past millennium. Geophysical Research Letters,
559 32(7).
560
561 Esper, J., Frank, D.C., Timonen, M., Zorita, E., Wilson, R.J., Luterbacher, J., Holzkämper, S.,
562 Fischer, N., Wagner, S., Nievergelt, D. and Verstege, A., 2012. Orbital forcing of tree-ring data.
563 Nature Climate Change, 2(12), pp.862-866.
564
565 Esper, J., Schneider, L., Smerdon, J.E., Schöne, B.R. and Büntgen, U., 2015. Signals and

566 memory in tree-ring width and density data. Dendrochronologia, 35, pp.62-70.
567
568 Frank, D., Esper, J. and Cook, E.R., 2007a. Adjustment for proxy number and coherence in a
569 large-scale temperature reconstruction. Geophysical Research Letters, 34(16).
570
571 Frank, D., Büntgen, U., Böhm, R., Maugeri, M. and Esper, J., 2007. Warmer early instrumental
572 measurements versus colder reconstructed temperatures: shooting at a moving target. Quaternary
573 Science Reviews, 26(25), pp.3298-3310.
574
575 Harris, I.P.D.J., Jones, P.D., Osborn, T.J. and Lister, D.H., 2014. Updated high-resolution grids
576 of monthly climatic observations–the CRU TS3. 10 Dataset. International Journal of
577 Climatology, 34(3), pp.623-642.
578
579 Luckman, B.H. and Wilson, R.J.S., 2005. Summer temperatures in the Canadian Rockies during
580 the last millennium: a revised record. Climate Dynamics, 24(2-3), pp.131-144.
581
582 Mantua, N.J., Hare, S.R., Zhang, Y., Wallace, J.M. and Francis, R.C., 1997. A Pacific
583 interdecadal climate oscillation with impacts on salmon production. Bulletin of the american
584 Meteorological Society, 78(6), pp.1069-1079.
585
586 McCarroll, D., Pettigrew, E., Luckman, A., Guibal, F. and Edouard, J.L., 2002. Blue reflectance
587 provides a surrogate for latewood density of high-latitude pine tree rings. Arctic, Antarctic, and
588 Alpine Research, pp.450-453.
589
590 Melvin, T.M., Briffa, K.R., Nicolussi, K. and Grabner, M., 2007. Time-varying-response
591 smoothing. Dendrochronologia, 25(1), pp.65-69.
592
593 Melvin, T.M. and Briffa, K.R., 2008. A “signal-free” approach to dendroclimatic standardisation.
594 Dendrochronologia, 26(2), pp.71-86.
595
596 Melvin, T.M. and Briffa, K.R., 2014. CRUST: Software for the implementation of Regional

597 Chronology Standardisation: Part 2. Further RCS options and recommendations.
598 Dendrochronologia, 32(4), pp.343-356.
599
600 Morice, C.P., Kennedy, J.J., Rayner, N.A. and Jones, P.D., 2012. Quantifying uncertainties in
601 global and regional temperature change using an ensemble of observational estimates: The
602 HadCRUT4 data set. Journal of Geophysical Research: Atmospheres, 117(D8).
603
604 Osborn, T.J., Biffa, K.R. and Jones, P.D., 1997. Adjusting variance for sample-size in tree-ring
605 chronologies and other regional-mean timeseries. Dendrochronologia, 15, pp.89-99.
606
607 Rohde, R., Muller, R.A., Jacobsen, R., Muller, E., Perlmutter, S., Rosenfeld, A., Wurtele, J.,
608 Groom, D. and Wickham, C., 2012. A new estimate of the average Earth surface land
609 temperature spanning 1753 to 2011. Geoinfor Geostat: An Overview, 1(1), pp.1-7.
610
611 Rydval, M., Larsson, L.Å., McGlynn, L., Gunnarson, B.E., Loader, N.J., Young, G.H. and
612 Wilson, R., 2014. Blue intensity for dendroclimatology: should we have the blues? Experiments
613 from Scotland. Dendrochronologia, 32(3), pp.191-204.
614
615 Rydval, M., Druckenbrod, D., Anchukaitis, K.J. and Wilson, R., 2015. Detection and removal of
616 disturbance trends in tree-ring series for dendroclimatology. Canadian Journal of Forest
617 Research, 46(3), pp.387-401.
618
619 Rydval, M., Loader, N.J., Gunnarson, B.E., Druckenbrod, D.L., Linderholm, H.W., Moreton,
620 S.G., Wood, C.V. and Wilson, R., 2017. Reconstructing 800 years of summer temperatures in
621 Scotland from tree rings. Climate Dynamics, pp.1-24.
622
623 Schneider, L., Smerdon, J.E., Büntgen, U., Wilson, R.J., Myglan, V.S., Kirdyanov, A.V. and
624 Esper, J., 2015. Revising midlatitude summer temperatures back to AD 600 based on a wood
625 density network. Geophysical Research Letters, 42(11), pp.4556-4562.
626
627 Schweingruber, F. 1988. Tree Rings: Basics and Applications of Dendrochronology. Springer,

628 NY.
629
630 Solomina, O.N., Bradley, R.S., Jomelli, V., Geirsdottir, A., Kaufman, D.S., Koch, J., McKay,
631 N.P., Masiokas, M., Miller, G., Nesje, A. and Nicolussi, K., 2016. Glacier fluctuations during the
632 past 2000 years. Quaternary Science Reviews, 149, pp.61-90.
633
634 Wigley, T.M., Briffa, K.R. and Jones, P.D., 1984. On the average value of correlated time series,
635 with applications in dendroclimatology and hydrometeorology. Journal of climate and Applied
636 Meteorology, 23(2), pp.201-213.
637
638 Wiles, G.C., D'Arrigo, R.D., Villalba, R., Calkin, P.E. and Barclay, D.J., 2004. Century-scale
639 solar variability and Alaskan temperature change over the past millennium. Geophysical
640 Research Letters, 31(15).
641
642 Wiles, G.C., D'Arrigo, R.D., Barclay, D., Wilson, R.S., Jarvis, S.K., Vargo, L. and Frank, D.,
643 2014. Surface air temperature variability reconstructed with tree rings for the Gulf of Alaska
644 over the past 1200 years. The Holocene, 24(2), pp.198-208.
645
646 Wilson, R.J. and Luckman, B.H., 2003. Dendroclimatic reconstruction of maximum summer
647 temperatures from upper treeline sites in Interior British Columbia, Canada. The Holocene,
648 13(6), pp.851-861.
649
650 Wilson, R., Rao, R., Rydval, M., Wood, C., Larsson, L.Å. and Luckman, B.H., 2014. Blue
651 Intensity for dendroclimatology: The BC blues: A case study from British Columbia, Canada.
652 The Holocene, 24(11), pp.1428-1438.
653
654 Wilson, R., K. Anchukaitis, K. Briffa, U. Büntgen, E. Cook, R. D' Arrigo, N. Davi, J. Esper, D.
655 Frank, B. Gunnarson, G. Hegerl, S. Klesse, P. Krusic, H. Linderholm, V. Myglan, Z. Peng, M.
656 Rydval, L. Schneider, A. Schurer, G. Wiles and E. Zorita. 2016. Last millennium northern
657 hemisphere summer temperatures from tree rings: Part I: The long term context. Quaternary
658 Science Reviews, 134, pp.1-18.

Wilson, R., Wilson, D., Rydval, M., Crone, A., Büntgen, U., Clark, S., Ehmer, J., Forbes, E., Fuentes, M., Gunnarson, B.E. and Linderholm, H.W., 2017. Facilitating tree-ring dating of historic conifer timbers using Blue Intensity. Journal of Archaeological Science, 78, pp.99-111.

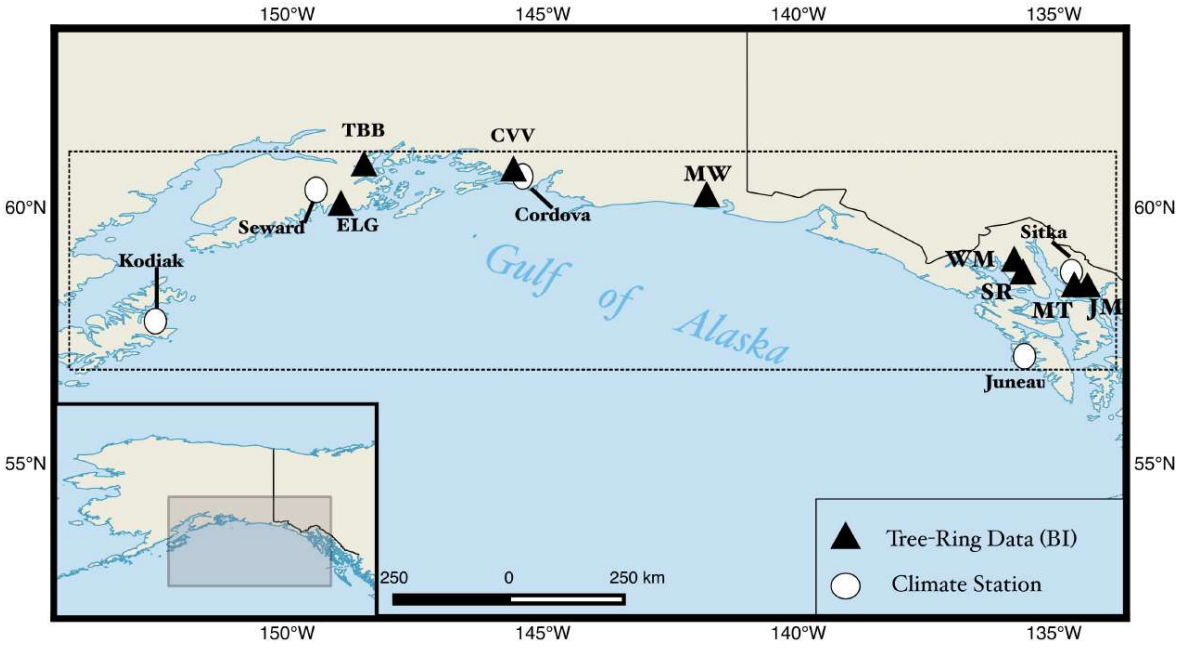

Figure 1: Location map of the eight GOA tree-ring sites used in this study (Table 1). Also indicated (dashed line box) is the domain (57-61°N / 153-134°W) of the gridded data (CRU TS 3.24, Harris et al. 2012; BEST, Rohde et al., 2012) used for calibration and the five coastal GOA temperature stations used in the original 5-station mean series (Wilson et al. 2007 – see supplementary Figure 1).

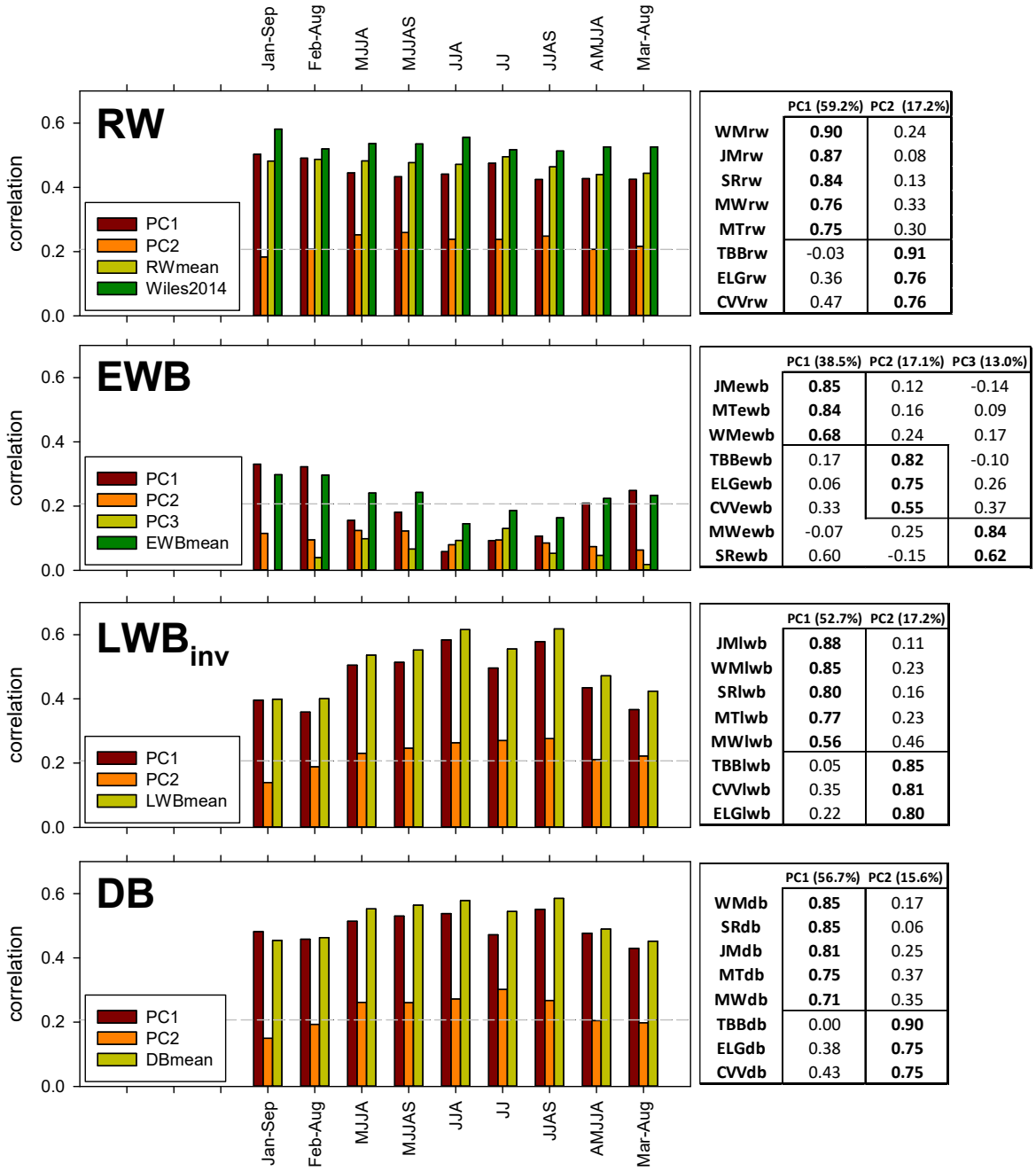

	PC1 (59.2%)	PC2 (17.2%)
WMrw	**0.90**	0.24
JMrw	**0.87**	0.08
SRrw	**0.84**	0.13
MWrw	**0.76**	0.33
MTrw	**0.75**	0.30
TBBrw	-0.03	**0.91**
ELGrw	0.36	**0.76**
CVVrw	0.47	**0.76**

	PC1 (38.5%)	PC2 (17.1%)	PC3 (13.0%)
JMewb	**0.85**	0.12	-0.14
MTewb	**0.84**	0.16	0.09
WMewb	**0.68**	0.24	0.17
TBBewb	0.17	**0.82**	-0.10
ELGewb	0.06	**0.75**	0.26
CVVewb	0.33	**0.55**	0.37
MWewb	-0.07	0.25	**0.84**
SRewb	0.60	-0.15	**0.62**

	PC1 (52.7%)	PC2 (17.2%)
JMlwb	**0.88**	0.11
WMlwb	**0.85**	0.23
SRlwb	**0.80**	0.16
MTlwb	**0.77**	0.23
MWlwb	**0.56**	0.46
TBBlwb	0.05	**0.85**
CVVlwb	0.35	**0.81**
ELGlwb	0.22	**0.80**

	PC1 (56.7%)	PC2 (15.6%)
WMdb	**0.85**	0.17
SRdb	**0.85**	0.06
JMdb	**0.81**	0.25
MTdb	**0.75**	0.37
MWdb	**0.71**	0.35
TBBdb	0.00	**0.90**
ELGdb	0.38	**0.75**
CVVdb	0.43	**0.75**

Figure 2: Left: Correlation response function analysis (1901-1989) using CRU TS3.24 mean temperatures with each tree-ring variable (RW = ring-width; EWB = early wood maximum blue intensity; LWB_{inv} = inverted latewood minimum blue intensity; DB – Delta Blue). The bars represent correlations with seasonal temperature for each principal component (PC) score and the simple GOA mean composite. Also for RW, correlations are shown for the Wiles et al. (2014) RW based RCS reconstruction. Horizontal line denotes the 95% confidence limit. Correlations against individual months are presented in Supplementary Figure 2. **Right:** Varimax rotation principal component analysis results showing loadings of each chronology on each PC with an eigenvalue > 1.0. % values denote the explained amount of variance each PC explains of the original data input matrix.

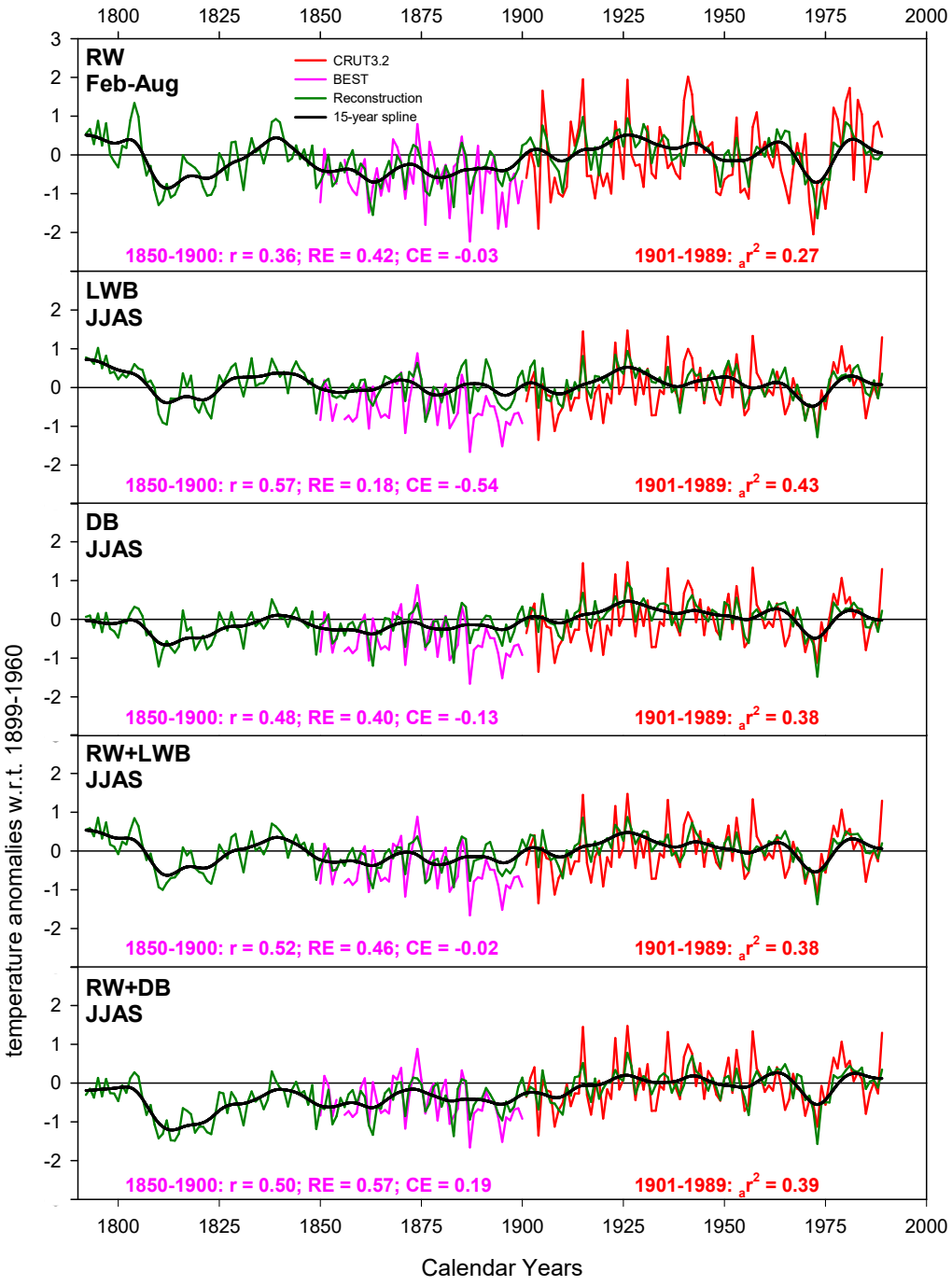

Figure 3: Illustration of the various PC regression experiments performed herein, with each reconstruction model compared against the June-September (Table 3). Feb-August is shown for RW as that was the reconstructed season in Wiles et al. (2014). Full period calibration is performed on the 1901-1989 period (Table 3 – CRU TS 3.24) while validation (Pearson's correlation coefficient (r), Reduction of Error (RE) and

693 Coefficient of Efficiency (CE)) is undertaken over 1850-1900 using the BEST gridded data after those data
694 were scaled to the CRU TS 3.24 data over the 1901-1989 period.
695
696

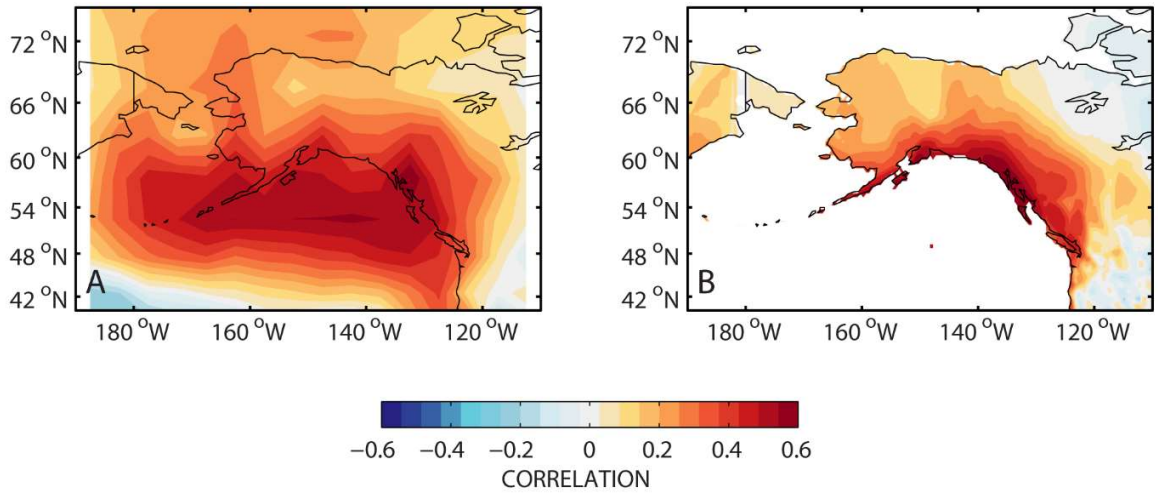

697

698 **Figure 4**: Spatial correlation (1901-1989) fields comparing the RW+DB GOA JJAS temperature reconstruction
699 with larger-scale temperatures. **A:** for HADCRUT4 land/SST (Morice et al. 2012; Cowtan and Way 2014); **B:** for
700 CRU TS3.24 land temperatures (Harris et al. 2012).

701
702

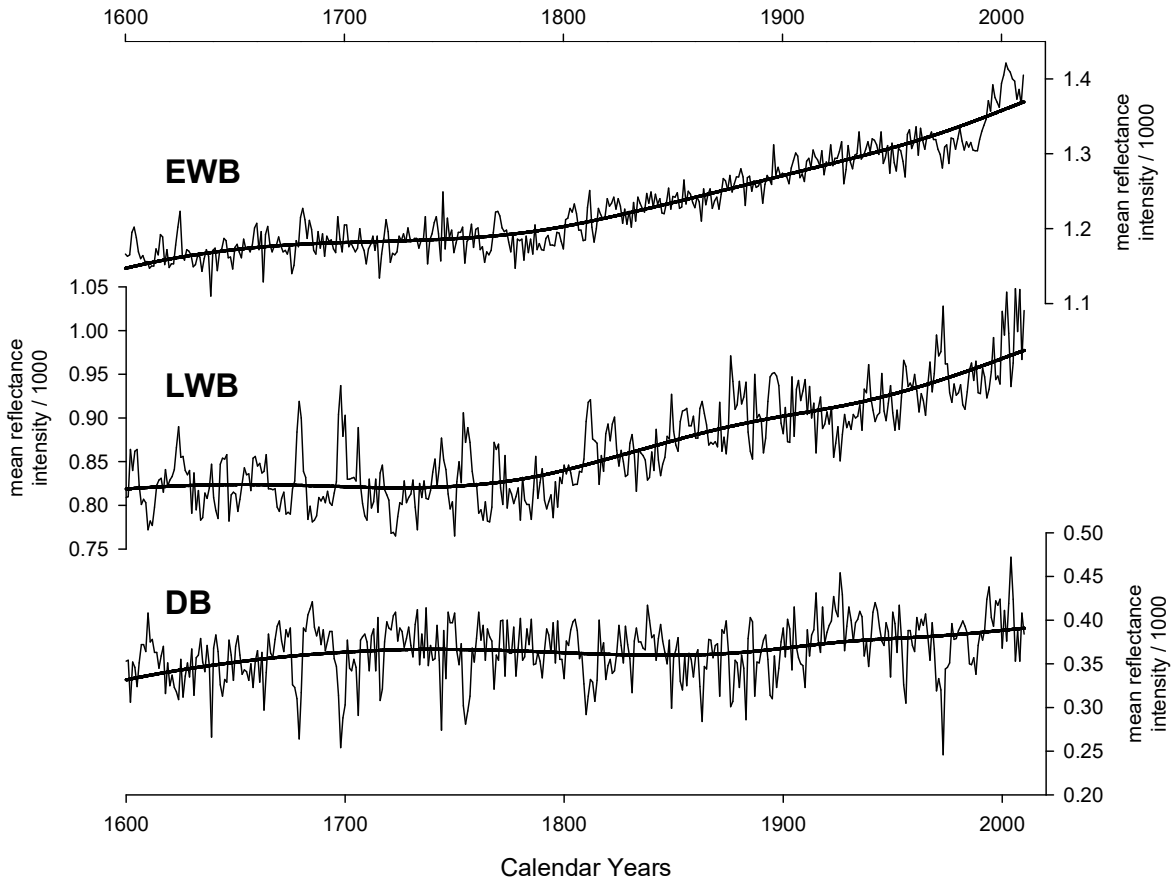

703

704

705 **Figure 5:** Mean non-detrended GOA wide composite chronologies since 1600 for EWB, LWB (non-inverted) and DB. The
706 LWB data have not been inverted for this figure.

707

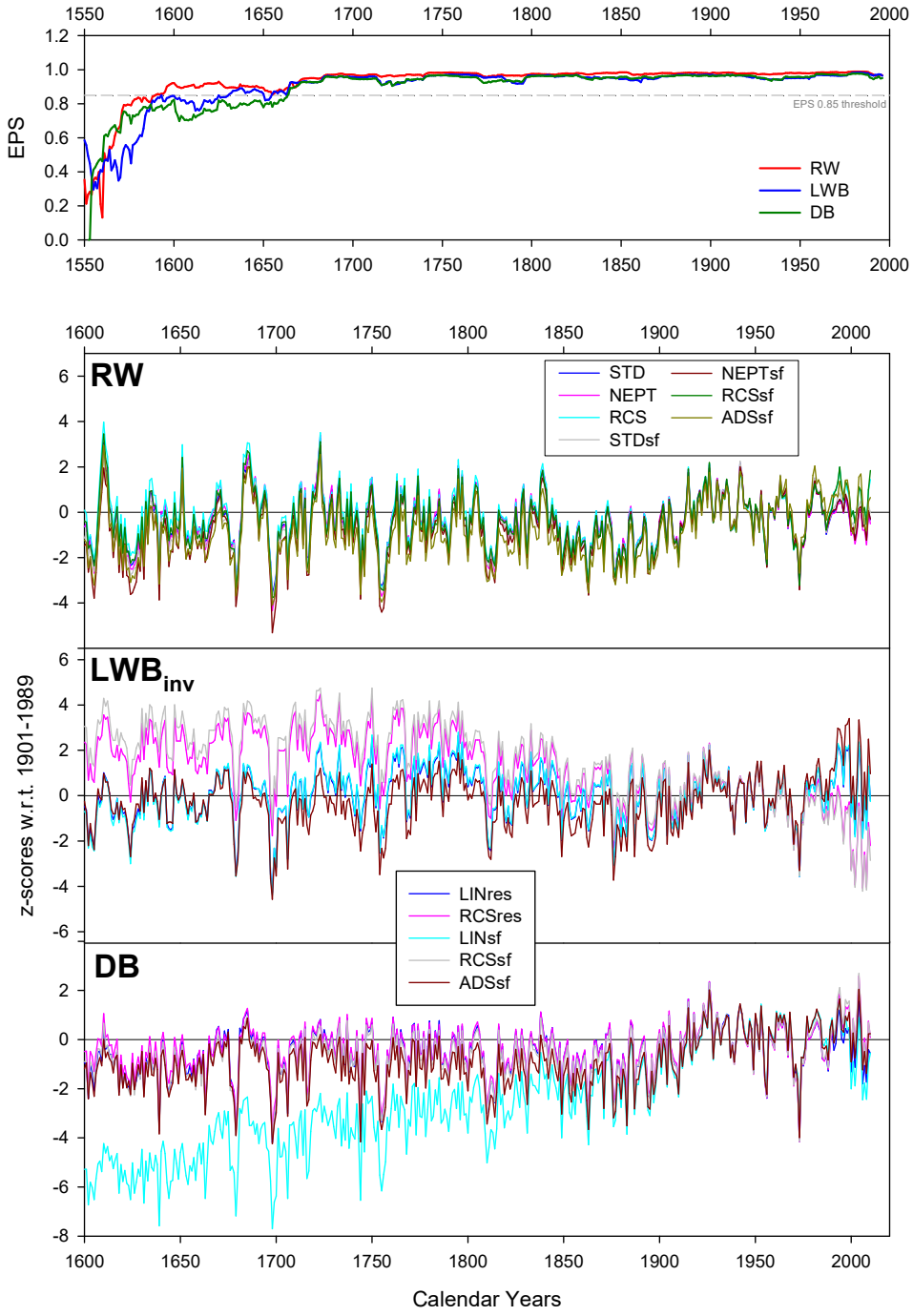

Figure 6: Detrending experiments for each TR variable using the full GOA regional composite (data from all 8 sites). Upper panel is 31-year moving EPS plots for RW, LWB_{inv} and DB using 200-yr spline detrending. Lower set of plots present chronology variants from 1600-2010. For RW - STD = negative exponential detrending (ratio) or regression function of zero or negative slope; NEPT = as STD but raw data have been power transformed and detrended via subtraction; RCS = single group RCS detrending (ratio); STDsf, NEPTsf, RCSsf = as previous three options but using signal free detrending; ADSsf = Age dependent spline detrending using signal free. For LWB_{inv} and DB – LINres – detrending via subtraction using linear functions (negative or zero

slope); RCSres = as RCS above but detrending via subtraction; LINsf and RCSsf = as with LINres and RCSres but with signal free detrending; ADSsf = Age dependent spline detrending using signal free.

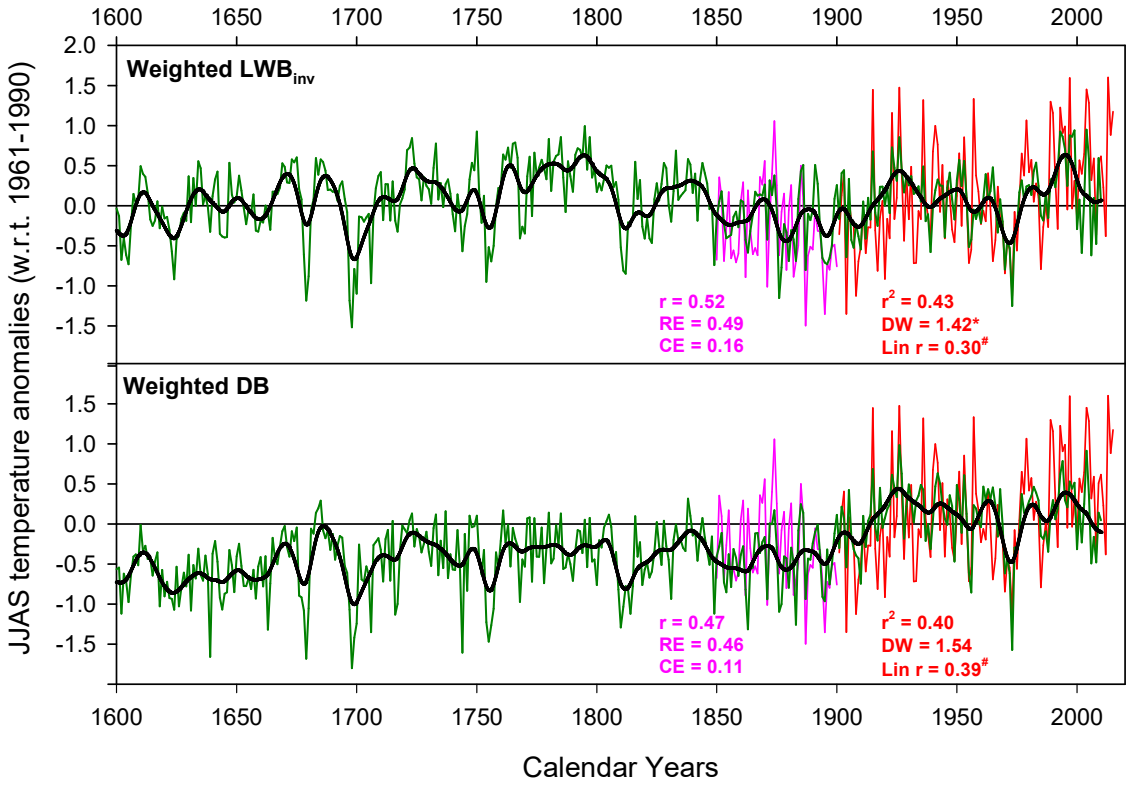

Figure 7: Extended reconstruction tests using LWB_{inv} and DB regional weighted averages. 1901-2010 period calibration uses CRU TS3.24 data (red) while validation is performed using BEST data (pink) over the 1850-1900 period. * denotes significant 1st order autocorrelation in model residuals; # denotes a significant linear trend in the model residuals. The smoothed functions are 15-year cubic smoothing splines.

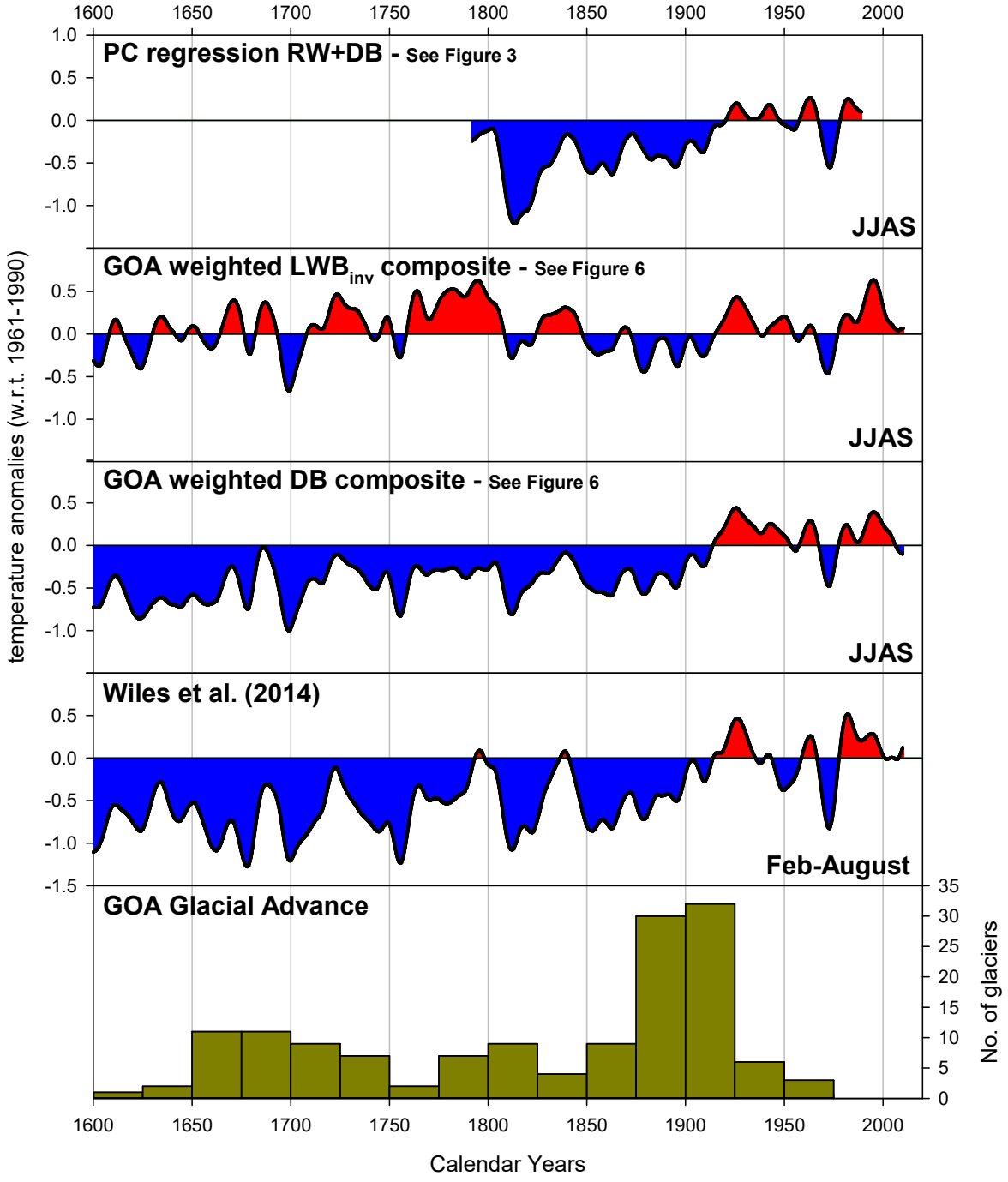

726

727

728 **Figure 8:** Comparison of GOA reconstruction variants using DB and RW with Wiles et al. (2014). The lower
729 panel presents a histogram of glacial advance in the GOA region (Wiles et al., 2004; Solomina et al. 2016).

730

Site Name	Timespan	No. of series	Period n > 5	MSL	RW RBAR	EWB RBAR	LWB RBAR	DB RBAR	N-RW EPS	N-EWB EPS	N-LWB EPS	N-DB EPS
Juneau Mtn (JM)	1558-1998	17	1604-1998	238.5	0.35	0.15	0.24	0.25	10.7	32.9	17.7	17.3
McGinnis (MT)	1485-1999	15	1584-1999	363.5	0.47	0.11	0.24	0.24	6.4	46.3	17.6	18.0
Son of Repeater (SR)	1713-2009	10	1792-2007	216.7	0.33	0.12	0.17	0.25	11.3	43.5	27.5	17.4
Wright Mtn (WM)	1610-2010	17	1738-2010	234.2	0.45	0.06	0.25	0.17	6.9	84.0	17.1	27.9
Miners Well (MW)	1479-1994	13	1640-1995	324.0	0.49	0.05	0.33	0.14	5.8	120.3	11.8	36.2
Cordova Eyak Mtn (CVV)	1573-1992	17	1672-1992	280.6	0.46	0.15	0.32	0.29	6.5	32.1	12.0	14.2
Tebenkof (TBB)	1357-1990	15	1605-1990	339.2	0.43	0.13	0.20	0.22	7.6	37.9	22.4	19.6
Ellsworth (ELG)	1636-1991	18	1750-1990	218.5	0.40	0.14	0.24	0.29	8.6	35.7	17.7	14.2
			median	259.6	0.44	0.12	0.24	0.24	7.23	40.70	17.62	17.69

Table 1: Metadata information for the eight GOA sites used in the study. The sites are ordered from east to west (see Figure 1). All PCA and related analyses were performed on the 1792-1990 period for which there is replication for all eight sites of at least five series. Tree-ring data were detrended using a 200-year spline for these signal strength analyses. The final 4 columns denote the number of series needed to attain an EPS of 0.85 (Wigley et al. 1984).

RW								
	JM	**MT**	**SR**	**WM**	**MW**	**CVV**	**TBB**	**ELG**
1850-1900	0.45	0.22	0.49	0.22	0.27	0.30	0.30	0.38
1901-1990	0.49	0.26	0.42	0.41	0.36	0.41	0.20	0.34
1850-1990	0.50	0.37	0.47	0.43	0.39	0.47	0.33	0.39
LWB_{inv}								
	JM	**MT**	**SR**	**WM**	**MW**	**CVV**	**TBB**	**ELG**
1850-1900	0.45	0.29	0.48	0.38	0.49	0.40	0.25	0.46
1901-1990	0.52	0.39	0.64	0.58	0.46	0.45	0.28	0.41
1850-1990	0.37	0.32	0.55	0.46	0.53	0.51	0.33	0.44
DB								
	JM	**MT**	**SR**	**WM**	**MW**	**CVV**	**TBB**	**ELG**
1850-1900	0.45	0.29	0.49	0.23	0.35	0.40	0.37	0.48
1901-1990	0.57	0.45	0.58	0.47	0.48	0.50	0.23	0.39
1850-1990	0.53	0.44	0.48	0.38	0.44	0.52	0.34	0.44

Table 2: Correlations (1850-1900, 1901-1990 and 1850-1990) for each site RW, LWB_{inv} and DB chronology against JJAS temperatures. EWB correlations are not shown. The sites are ordered from east to west (see Figure 1).

mean r	**RW**	**EWB**	**LWB_{inv}**	**DB**
RW		0.27	0.68	0.81
EWB			-0.23	0.36
LWB_{inv}				0.80
DB				

Table 3: Correlation matrix between the different tree-ring variable chronologies (200-year spline detrended. These values represent the averages for between TR variable correlations performed separately for each site.

		1901-1960 Calibration			1961-1989 Validation			1901-1989 Full Calibration + Residuals			
Wiles14	**season**	**series entered**	**r**	**r2**	**r**	**RE**	**CE**	**r**	**r2**	**DW**	**Linr**
	MJJA	Wiles2014	0.60	0.36	0.48	0.11	0.10	0.55	0.30	1.62	0.15
	MJJAS	Wiles2014	0.55	0.30	0.53	0.21	0.20	0.53	0.28	1.72	0.17
	JJA	Wiles2014	0.58	0.34	0.47	0.06	0.05	0.53	0.28	1.75	0.17
	JJAS	Wiles2014	0.52	0.27	0.53	0.20	0.20	0.51	0.26	1.77	0.18
	Feb-Aug	Wiles2014	0.60	0.36	0.54	0.23	0.23	0.57	0.33	1.78	0.17
RW	**season**	**PCs entered**	**r**	**ar2**	**r**	**RE**	**CE**	**r**	**ar2**	**DW**	**Linr**
	MJJA	1, 2	0.60	0.34	0.40	0.03	0.03	0.52	0.26	1.60	0.21
	MJJAS	1, 2	0.56	0.29	0.46	0.15	0.14	0.52	0.25	1.70	0.23
	JJA	1, 2	0.58	0.31	0.42	-0.01	-0.02	0.51	0.24	1.74	0.23
	JJAS	2, 1	0.53	0.26	0.49	0.16	0.15	0.51	0.24	1.76	0.24
	Feb-Aug	2, 1	0.60	0.36	0.46	0.08	0.08	0.54	0.27	1.75	0.23
LWB_{inv}	**season**	**PCs entered**	**r**	**ar2**	**r**	**RE**	**CE**	**r**	**ar2**	**DW**	**Linr**
	MJJA	1, 2	0.63	0.38	0.49	0.15	0.14	0.57	0.31	1.39	0.20
	MJJAS	1, 2	0.63	0.37	0.55	0.23	0.22	0.59	0.34	1.50	0.23
	JJA	1, 2	0.71	0.49	0.58	0.16	0.15	0.66	0.42	1.45	0.25
	JJAS	1, 2	0.69	0.46	0.64	0.27	0.27	0.66	0.43	1.51	0.27
DB	**season**	**PCs entered**	**r**	**ar2**	**r**	**RE**	**CE**	**r**	**ar2**	**DW**	**Linr**
	MJJA	1, 2	0.69	0.45	0.43	-0.01	-0.02	0.59	0.33	1.55	0.24
	MJJAS	1, 2	0.67	0.43	0.50	0.09	0.08	0.61	0.37	1.68	0.26
	JJA	1, 2	0.70	0.47	0.50	-0.05	-0.05	0.62	0.36	1.65	0.26
	JJAS	1, 2	0.68	0.44	0.58	0.11	0.11	0.63	0.38	1.72	0.29
RW + LWB_{inv}	**season**	**PCs entered**	**r**	**ar2**	**r**	**RE**	**CE**	**r**	**ar2**	**DW**	**Linr**
	MJJA	1, 2	0.69	0.45	0.46	0.03	0.03	0.60	0.34	1.67	0.18
	MJJAS	1, 2	0.66	0.43	0.51	0.13	0.12	0.62	0.37	1.87	0.20
	JJA	1, 2, 3	0.72	0.49	0.52	-0.07	-0.08	0.63	0.37	1.56	0.26
	JJAS	1, 2, 3	0.68	0.43	0.59	0.12	0.12	0.63	0.38	1.63	0.28
RW + DB	**season**	**PCs entered**	**r**	**ar2**	**r**	**RE**	**CE**	**r**	**ar2**	**DW**	**Linr**
	MJJA	1, 2	0.71	0.49	0.44	-0.16	-0.16	0.62	0.36	1.69	0.04
	MJJAS	1, 2	0.72	0.51	0.49	-0.14	-0.15	0.61	0.36	1.78	-0.11
	JJA	1, 2, 3	0.72	0.50	0.49	-0.15	-0.15	0.56	0.32	1.89	-0.12
	JJAS	1, 2	0.71	0.49	0.52	-0.18	-0.18	0.64	0.39	1.84	0.05

Table 4: Calibration experiments for the four strongest seasons (see Figure 2). Initial calibration (using CRU TS 3.24) was made over 1901-1960 and validation over 1961-1989. Full calibration (1901-1989) was also performed to allow for residual tests and extra validation using BEST (1850-1990 – see Figure 2). Shaded results do not pass significance. r = Pearson's correlation coefficient; r2 = coefficient of determination; ar2 = r2 adjusted for the number of predictors in the model; RE = Reduction of Error; CE = Coefficient of Efficiency; DW = Durbin-Watson test for residual autocorrelation; LINr = linear trend of the residuals.

	1901-2010 Calibration					1850-1900 Validation		
	series entered	**r**	**r2**	**DW**	**LINr**	**r**	**RE**	**CE**
LWB_{inv}	LINres	0.64	0.41	1.36	0.36	0.53	0.44	0.07
	RCSres	0.26	0.07	1.28	0.48	0.56	0.01	-0.64
	LINsf	0.64	0.41	1.37	0.36	0.53	0.43	0.06
	RCSsf	0.21	0.05	1.32	0.46	0.56	-0.05	-0.73
	ADSsf	0.69	0.47	1.58	0.06	0.50	0.51	0.20
	1901-2010 Calibration					1850-1900 Validation		
	series entered	**r**	**r2**	**DW**	**LINr**	**r**	**RE**	**CE**
DB	LINres	0.55	0.31	1.37	0.50	0.50	0.52	0.21
	RCSres	0.64	0.40	1.59	0.40	0.48	0.50	0.18
	LINSF	0.54	0.29	1.35	0.38	0.43	0.40	0.00
	RCSsf	0.65	0.43	1.64	0.35	0.47	0.48	0.15
	ADSsf	0.65	0.42	1.59	0.30	0.47	0.34	-0.09

Table 5: Extended reconstruction calibration experiments using different chronology versions (Figure 6) of LWB_{inv} and DB. Shaded results do not pass significance.